Received: 20 April 2017 | Accepted: 25 April 2017

DOI: 10.1002/cne.24236

RESEARCH ARTICLE

WILEY The Journal of Comparative Neurology

Innervation of the syrinx of the zebra finch (*Taeniopygia guttata*)

Macarena Faunes | João F. Botelho | J. Martin Wild

Department of Anatomy and Medical Imaging, Faculty of Medical and Health Sciences, University of Auckland, Auckland, New Zealand

Correspondence
J. Martin Wild, Department of Anatomy and Medical Imaging, Faculty of Medical and Health Sciences, University of Auckland, Private Bag 92019, Grafton 1023, Auckland, New Zealand.
Email: jm.wild@auckland.ac.nz

Funding information
NIH, Grant/Award Number: RO1NS029467; HFSP, Grant/Award Number: RPG0012/2010

Abstract

In songbirds, the learning and maintenance of song is dependent on auditory feedback, but little is known about the presence or role of other forms of sensory feedback. Here, we studied the innervation of the avian vocal organ, the syrinx, in the zebra finch. Using a combination of immunohistochemistry, immunofluorescence and neural tracing with subunit B of cholera toxin (CTB), we analysed the peripheral and central endings of the branch of the hypoglossal nerve that supplies the syrinx, the tracheosyringeal nerve. In the syringeal muscles, we show the presence of numerous choline acetyl transferase-like immunoreactive *en plaque* motor endplates and substance P-like immunoreactive, thin and varicose free nerve endings. Substance P-like immunoreactive free nerve endings were also present in the luminal syringeal tissues, especially in the luminal epithelium of the trachea and pessulus. Also, by a combination of immunofluorescence and transganglionic tracing following injections of CTB in the tracheosyringeal nerve, we identified as central targets of the syringeal receptors the caudolateral part of the interpolaris subnucleus of the descending trigeminal tract, a caudolateral region of the nucleus tractus solitarius, and a lateral band of the principal sensory trigeminal nucleus. Further studies are required to determine the sensory modalities of these receptors and the connections of their specific synaptic targets.

KEYWORDS
somatosensory feedback, songbirds, RRID: AB_10000347, RRID: AB_10000320, RRID: AB_10013220, RRID: AB_2079751, RRID: AB_2532998, RRID: AB_10000343, AB_396357, RRID: SCR_00177

1 | INTRODUCTION

Beyond its outstanding beauty, the singing of songbirds has attracted the attention of scientists as a complex behavior learned by imitation (Marler, 2004). As a central component of social interactions, and particularly of courtship, this behavior has presumably been critical in speciation events throughout the history of songbirds (Grant & Grant, 2010). Furthermore, the learning of song by songbirds parallels to a certain extent the learning of speech by humans (Doupe & Kuhl, 1999; Marler, 1970). Much of the scientific interest in songbirds has focused on the central neural circuits involved in the learning and motor control of singing (Schmidt & Wild, 2014; Wild, 2004, 2008), and important advances have been made in recent years in our understanding of the mechanisms of sound production in the avian vocal organ, the syrinx, and its peripheral control (Elemans, 2014; Fee, Shraiman, Pesaran, & Mitra, 1998; Goller & Cooper, 2004; Goller & Larsen, 1997; Suthers & Zollinger, 2004). However, the presence of somatosensory feedback from the syrinx and its possible role in singing has received little attention (Bottjer & Arnold, 1982), a situation that could be alleviated by a more detailed description of syringeal innervation than presently available.

The syrinx is a specialisation of the junction between the trachea and the bronchi (Figure 1a–f). Its structure is highly variable among species, and has been extensively used as a character for phylogenetic analyses (Ames, 1971; King, 1989; Prum, 1992). In songbirds, the tracheo- and bronchio-syringeal skeleton is highly modified. In the zebra finch, four to six of the caudal most tracheal rings and the first pair of bronchial rings are fused into a structure called the tympanum, and the rostral bronchial semi-rings are flattened (Düring et al., 2013). The luminal side of the syringeal skeleton is covered with tissues rich in collagen, elastic fibers, and glycosaminoglycans (Riede & Goller, 2010). These tissues form two pairs of labia at the level of the bronchial modified semi-rings, which produce sound as the expiratory airflow causes them to vibrate (Goller & Larsen, 1997). Outside the syringeal skeleton,

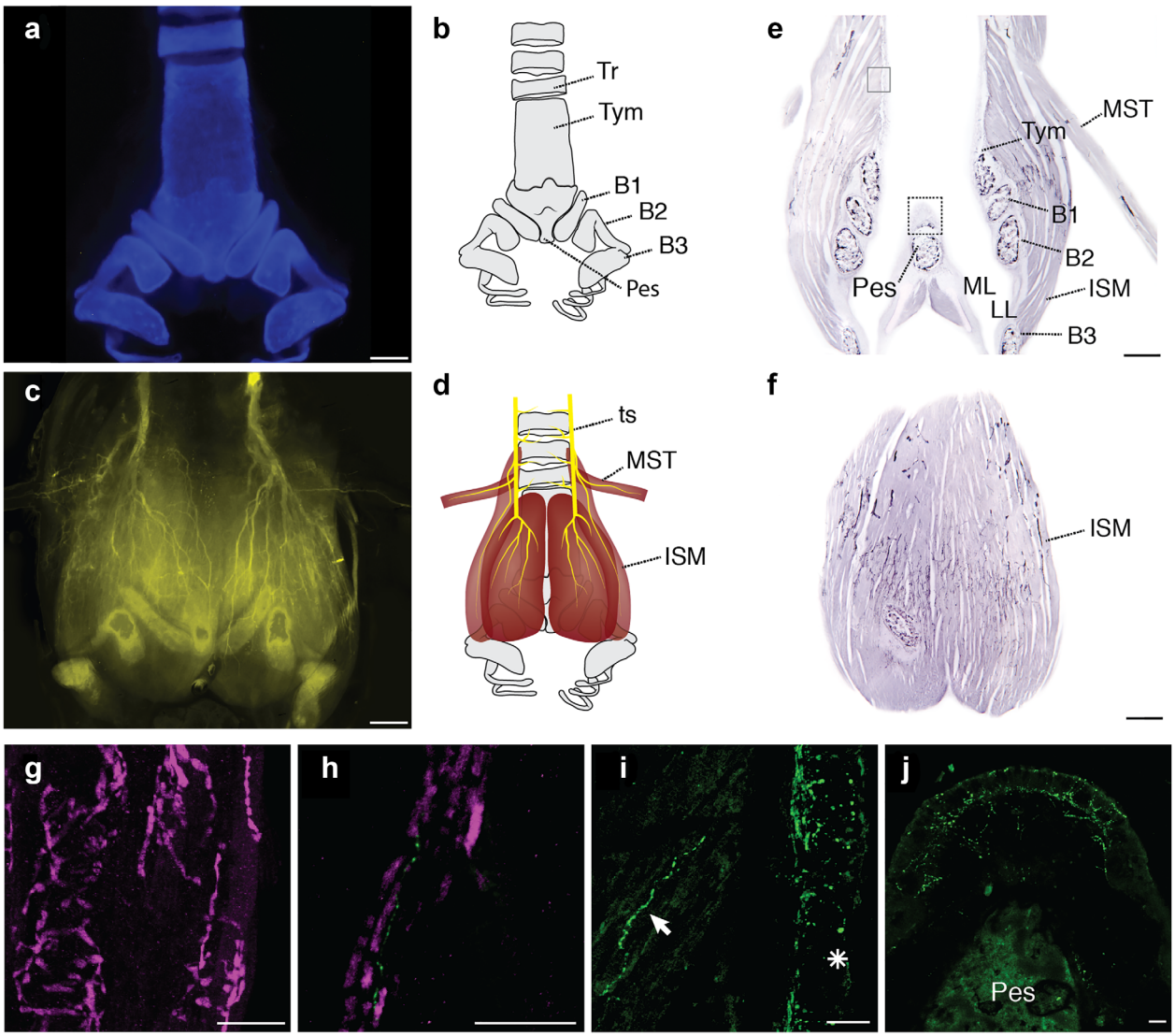

FIGURE 1 Innervation of the syrinx of the zebra finch. (a) Ventral view of a whole-mounted syrinx cleared with a clarity-like procedure and stained with calcein (pseudo-colored blue) to show its skeletal elements. (b) Schematic representation of the syringeal skeletal elements. (c) Ventral view of a whole-mounted syrinx cleared with a clarity-like procedure and stained with immunofluorescence against neurofilament (pseudo-colored yellow) to visualize its innervation. (d) Schematic representation of the syringeal musculature and its innervation. (e, f) Immunohistochemistry against neurofilament in coronal sections of a syrinx (middle and ventral levels, respectively). Staining of the sectioned skeletal elements is nonspecific and occurs even in the absence of primary antibody incubation. Squares in (e) depict the location of photomicrographs in panels (i) and (j) (see below). (g–j) Confocal photomicrographs of coronal sections of a syrinx stained with immunofluorescence against ChAT (pseudo-colored magenta) and substance P (green) in the syringeal muscles (g–h), and in regions equivalent to those pointed in panel (e) by solid (i) and dashed (j) line squares. In the syringeal muscles (g, h, and arrow in i), there are ChAT-like immunoreactive motor endplates and thin substance P-like immunoreactive varicose nerve fibers. Thin substance P-like immunoreactive fibers and fiber endings are also found in the luminal wall of the trachea (asterisk in i), and in the tissue luminal to the pessulus (j). B1, B2, B3 = bronchial semirings 1, 2, and 3; ISM = intrinsic syringeal muscles; LL = lateral labium; ML = medial labium; MST = sternotrachealis muscle; Pes = pessulus; Tr = tracheal ring; ts = tracheosyringeal nerve; Tym = tympanum. Scale bars in (a), (c), (e), and (f) = 500 μm. Scale bars in (g–j) =25 μm

there are several pairs of muscles that can originate and insert on the trachea, tympanum, bronchial semi-rings and bronchial cartilages, and are able to independently modify the tension and degree of adduction of the two pairs of labia, thus modulating the acoustic frequencies produced on each side. Such muscles, with both origin and insertion within the syrinx, are called intrinsic syringeal muscles (King, 1989). Other muscles, connecting the syrinx to other structures such as the sternum or the larynx, are called the extrinsic syringeal muscles, and in songbirds they are thought to stabilise the organ during song production (Düring et al., 2013; Goller & Suthers, 1996).

The syringeal muscles are innervated by motoneurons in the tracheosyringeal part of the hypoglossal motor nucleus (nXII ts), which receives a direct projection from the telencephalic nucleus robustus of the arcopallium, the premotor forebrain nucleus of the song system (Nottebohm, Stokes, & Leonard, 1976). The syringeal motoneurons send their axons to the syrinx through the tracheosyringeal hypoglossal

nerve (ts nerve). Through this nerve also travel afferent fibers of cell bodies located in the jugular vagal ganglion, the central projections of which project to the trigeminal sensory complex together with lingual hypoglossal afferents (Bottjer & Arnold, 1982; Faunes & Wild, 2017a; Wild, 1981, 1990). However, the sensory endings of the syringeal receptors have not yet been described, and their specific trigeminal targets have not been distinguished from the lingual afferent terminal fields. The lack of detail concerning the syringeal projections may be due to technical difficulties associated with transganglionic transport of the tracers used (Bottjer & Arnold, 1982; Wild, 1981).

In the present work, we use a combination of immunostaining and tract tracing with the sensitive neural tracer subunit B of cholera toxin (CTB) to describe the morphology and location of motor and sensory nerve endings in the syrinx of the zebra finch, and to identify the specific central targets of the syringeal receptors.

2 | METHODS

A total of 19 adult male zebra finches were used exclusively for this study. Additionally, syringes from another 10 animals that had been perfused for unrelated studies, were used for immunostaining. All procedures were approved by the Animal Ethics Committee of the University of Auckland.

2.1 | Tracer injections in the tracheosyringeal nerve

The animals were anesthetised with an intramuscular injection of an equal parts mixture of ketamine and xylazine (50 mg/kg and 20 mg/kg, respectively) and placed in supine position in a custom-made stereotaxic frame with ear and beak bars. The neck was extended to expose the throat and a longitudinal midline incision gave access to the trachea and the ts nerve (usually the right one) that accompanies it on either side. A piece of parafilm (Sigma Aldrich, St. Louis, MO) was placed underneath the nerve to make it taut, and a few drops of melted paraffin wax (42°C melting point) were placed on top of it to prevent its desiccation during the injection procedure. A glass micropipette (World Precision Instruments, Sarasota, FL, 1B150F-4) having a tip outer diameter of 20–25 μm was connected to a pressure pulse source (picospritzer, Parker, Hollis, NH) and used to inject beta subunit of cholera toxin (CTB, Sigma Aldrich, Cat. # C167-500UG, Lot#SLBK3733V, 1% in PBS; 10 animals) into the ts nerve. The parafilm was then removed and the surgical incision closed. The animals were left to recover from anesthesia and survive for 1–3 days to allow transport of the tracer before tissue processing.

2.2 | Tracer injections in the brainstem

The procedure for brainstem injections is described in an accompanying article (Faunes & Wild, 2017b). Briefly, the animals were anesthetised as described above and fixed in the stereotaxic frame with the beak angled down with respect to the horizon so that the confluence of the mid-sagittal and cerebellar sinuses ("Y" point) was 0.3 mm caudal to inter-aural zero. Coordinates to reach the nuclei of the descending trigeminal tract (nTTD), the nucleus tractus solitarius (nTS), and the principal trigeminal nucleus (PrV; three animals per target) were obtained from an unpublished stereotaxic atlas of the zebra finch brain (courtesy of Dr. M. Konishi) and guided by extracellular recordings. The trigeminal sensory nuclei were identified using responses to light touch of the beak with a paintbrush, and the position of nTS was inferred from its distance from the cerebellum, which could be identified on the basis of its characteristic spontaneous activity and, at deep levels, from its visually evoked activity. After performing an incision in the scalp and a small craniotomy, tungsten microelectrodes (2–4 MΩ, Frederick Haer, Inc., Bowdoin, ME) were placed using an X-Y stage (460A-XY, Newport, Irvine, CA) and advanced into the brain with a Micro-Positioning Controller (MC-5B, National Aperture, Inc., Salem, NH). In order to avoid the bone that covers the dorsolateral aspect of the medulla, the electrodes were placed at lateral angles ranging between 13° and 15° to reach the nTTD and PrV from a craniotomy located at the midline. To reach nTS, the electrodes were lowered vertically. Electrophysiological signals were amplified and filtered between 100 Hz and 10 KHz with a two-channel differential AC amplifier (AM systems, Model 1800, Sequim, WA), and monitored with a digital oscilloscope (TDS 2014, Tektronix, Beaverton, OR) and a loud speaker (MS2, Tucker Davis Technologies, Inc., Alachua, FL). The tungsten micro-electrodes were then replaced by tracer-filled glass micropipettes. The tracer was delivered by iontophoresis (2–4 microamps positive current, 7 s on–off cycle for a total of 15–20 min) and/or air pressure. After the injections were placed, the pipettes were retracted, the surgical incision closed, and the animals were left to recover from anesthesia and survive for 2–4 days to allow transport of the tracer before tissue processing.

2.3 | Tissue processing

The animals were anesthetised as described above and transcardially perfused with 0.9% saline and 4% paraformaldehyde (PFA). After >4 hr post fixation in 4% PFA, the brain and syringes were removed, and the brains were blocked in the coronal plane in the stereotaxic frame. Then, brains and syringes were placed in 30% sucrose buffer until they sank (usually 8 hr), embedded in 12% gelatin, postfixed again for 2 hr, placed in 30% sucrose until they sank again, and sectioned on a freezing microtome. Syringes and brains were sectioned in the coronal plane at 45 and 35 microns, respectively (i.e., the syringes were sectioned lengthwise). Sections were collected serially in PBS in two or three alternating series.

2.4 | Antibodies characterisation

Primary antibodies used in this study are listed in Table 1. Calbindin, calretinin, and parvalbumin are calcium-binding proteins often used as neuroanatomical markers (Braun, 1990). Substance P is a neuropeptide often expressed in the somata and terminals of primary sensory neurons (Hokfelt, Kellerth, Nilsson, & Pernow, 1975). Choline acetyl transferase (ChAT) is the synthetic enzyme for acetylcholine, and it is found in the soma, dendrites, and axon of cholinergic neurons (Houser, Crawford, Barber, Salvaterra, & Vaughn, 1983). Neurofilament M is one of

TABLE 1 List of antibodies used in this study

Antigen	Description of immunogen	Vendor, host species, cat. #, clone or lot #, RRID	Concentration/dilution used	
			Immunohistochemistry	Immunofluorescence
Calbindin D-28k	Calbindin D-28k purified from chicken duodenum	Swant, mouse, 300, 07 (F), AB_10000347	1:5,000	–
Calretinin	Human recombinant calretinin-22k	Swant, mouse, 6B3, 010399, AB_10000320	1:5,000	–
Cholera toxin B Subunit	Purified cholera toxin B subunit from Vibrio cholerae type inaba 569B	List Biological, goat, 703, 7032A6, AB_10013220	1:33,000	1:33,000
Choline Acetyltransferase	Choline Acetyltransferase, human placental enzyme	Millipore, goat, AB144P, 2603400, AB_2079751	5 μg/ml	20 μg/ml
Neurofilament-M	Neurofilament-M See NCBI gene	Thermo Fisher Scientific, mouse, 13-0700, 810165A, AB_2532998	1:1,000	1:500 (sections) 1:100 (whole-mount)
Parvalbumin	Carp muscle carp II parvalbumin conjugated to tetanus toxoid	Swant, mouse, 235, Lot 10-11 (F), AB_10000343	1:5,000	–
Substance P	Substance P	BD Biosciences, rat, 556312, 5079983, AB_396357	1:10,000	1:3,000

the subunits of the intermediate filaments of the cytosketeton of neurons, and can be used to label nerves (Hirokawa, Glicksman, & Willard, 1984).

Characterisation of the anti-calbindin D-28k (Swant, Switzerland, made in mouse, Cat. #300, Lot. #07 (F), RRID AB_10000347), anti-cholera toxin B subunit (List Biological, Campbell, CA, made in goat, Cat. #703, Lot. #7032A6, RRID AB_10013220), and anti-substance P (BD Biosciences, San Jose, CA, made in rat, Cat. #556312, Lot. #5079983, RRID AB_396357) antibodies is described in an accompanying article (Faunes & Wild, 2017a).

The anti-calretinin antibody (Swant, made in mouse, Cat. #6B3, Lot- #010399, RRID AB_10000320) was developed and characterized by Zimmermann and Schwaller (2002). The hybridoma cell line was obtained from mice previously immunised with human recombinant calretinin-22k. This antibody stains a band corresponding to the molecular weight of calretinin in western blot of brain extracts from various vertebrate species, including chicken, zebrafish, and some mammals (Zimmermann & Schwaller, 2002).

The anti-ChAT polyclonal antibody (Millipore, Billerica, MA, made in goat, Cat. #AB144P, Lot. #2603400, RRID AB_2079751) was raised against the human placental enzyme. This antibody was characterized by Stensrud, Chaudhry, Leergaard, Bjaalie, and Gundersen (2013) with western blot of rat brain lysate, where it stains a single band at 68–70 kD.

The anti-neurofilament-M antibody (Thermo Fisher Scientific, Waltham, MA, made in mouse, Cat. #13–0700, Lot. #810165A, RRID AB_2532998) was developed by Lee, Carden, Schlaepfer, and Trojanowski (1987). The hybridoma cell line was obtained from mice previously immunised with neurofilament-M extracted from rat spinal cord (Lee et al., 1987). This antibody stains a single band at 150 kD from cytoskeletal protein fractions extracted from mouse spinal cord and sciatic nerve (Yan, Jensen, & Brown, 2007).

The anti-parvalbumin antibody (Swant, made in mouse, Cat. #235, Lot. #10-11 (F), RRID AB_10000343) was developed by Celio, Baier, Schärer, De Viragh, and Gerday (1988). The hybridoma cell line was obtained from mice previously immunised with parvalbumin extracted from carp muscle, conjugated to tetanus toxoid. In two-dimensional immunoblot of rat cerebellum, this antibody stains a calcium binding spot in the12kD and pI 14.9, identical to purified parvalbumin (Celio et al., 1988).

2.5 | Immunohistochemistry

Immunohistochemistry against CTB, ChAT, calbindin, calretinin, parvalbumin and substance P was performed as described in an accompanying article (Faunes & Wild, 2017a). All incubation steps were done at room temperature with gentle agitation on an orbital shaker and preceded by PBS washes (3x 10 min), and for all antibodies some brain sections were included as positive controls for staining. First, the sections were incubated for 15 min in a solution of 0.3% H_2O_2 and 50% methanol in PBS to quench endogenous peroxidase activity. Then, they were incubated overnight in a primary antibody diluted as listed in Table 1 in a blocking solution consisting of 0.4% Triton X-100 and 2% normal donkey serum (Sigma Aldrich, Cat. # D9663, Lot# SLBL4004V) in PBS. Next, sections were incubated for 1 hr in secondary antibody (biotinylated rabbit anti-rat, Life Technologies, Carlsbad, CA, Cat# A18919, Lot#38–59-122313; biotinylated donkey anti-goat, Jackson Immuno, Cat# 705-065-003, Lot# 67132; or biotinylated donkey anti-mouse, Jackson Immuno West Grove, PA, Cat# 715-065-150, Lot# 87909) diluted 1:500 in blocking solution, and then for 1 hr in horseradish peroxidase (HRP)-conjugated neutravidin (Thermo Fisher Scientific, CA# 31001, Lot# QE317304) diluted 1:1000 in 0.4% triton PBS. Finally, sections were incubated in a solution of 0.25mg/ml diamonobenzidine hydrochloride (DAB), 0.2 mg/ml $CoCl_2$ in PBS (to produce a black reaction product), to which a few drops of 0.3% H_2O_2 were added to start the DAB-peroxidase reaction. The reaction was

stopped after 1–3 min by transferring the sections to PBS. The sections were mounted in gelatin-coated slides and left to dry, then cleared in an ascending series of ethanol followed by xylene and coverslipped with DPX mounting medium (Sigma Aldrich).

2.6 | Immunofluorescence in sections

Immunofluorescence for detection of CTB, ChAT and substance P was performed as described in an accompanying article (Faunes & Wild, 2017a). All incubation steps were done using gentle agitation and preceded by PBS washes (3x 10 min). Sections were incubated in one or two primary antibodies diluted as listed in Table 1 in the blocking solution described above, for 60 hr at 4°C. Then, they were incubated for 2 hr at room temperature in one or two secondary antibodies (biotinylated donkey anti-goat, Jackson Immuno, Cat# 705-065-003; Alexa Fluor 488 conjugated rabbit anti-rat, Life Technologies, Cat# A21210, Lot# 1717038) diluted 1:500 in blocking solution. For immunostaining involving anti- ChAT or CTB primary antibodies, a third incubation step in Dylight 594 conjugated neutravidin (Thermo Fisher Scientific, Cat#22842, Lot#QF222109) at room temperature for 1 hr was added. Sections were mounted and coverslipped with Vectashield (Vector Labs, Burlingame, CA) mounting medium.

2.7 | Immunofluorescence and calcium staining in whole mount syringes

We followed the procedure for whole mount clearing and immunostaining from Botelho et al. (2017). Syringes were extracted from animals perfused with 4% PFA and saline, washed in cold PBS and then incubated with gentle agitation for 2 days at 4°C in a modified version of Clarity fixative (PFA 4%, 2% Acrylamide, 1% VA-044 Initiator in PBS) (Tomer, Ye, Hsueh, & Deisseroth, 2014). Next, the tubes containing the syringes were placed in a dissection chamber where the air was replaced by nitrogen to trigger polymerisation. Then, the tubes were closed and left to polymerize in gentle agitation for 2 hr at 37°C. Next, the syringes were incubated in 4% sodium dodecyl sulfate (SDS) in boric acid buffer pH 8.5 for 1 week to remove their lipids. For calcium labeling, the cleared syringes were incubated using gentle agitation for 2 hr at room temperature in 0.002% calcein in PBS. For immunofluorescence, cleared syringes were incubated in primary antibody anti-neurofilament (Thermo Fisher Scientific, made in mouse, Cat# 13-0700, Lot# 810165A, RRID AB_2532998) diluted as listed in Table 1 in 5% donkey serum, 5% dimethyl sulfoxide (DMSO), 0.1% sodium azide in PBS at 37°C for 48 hr, followed by Alexa Fluor 546 donkey anti-mouse secondary antibody (Invitrogen Carlsbad, CA, Cat# A10036, Lot# 1458642) diluted 1: 200 in 5% donkey serum, 5% DMSO in PBS and incubated for at 37°C for 24 hr.

2.8 | Data analysis and image processing

The sections were examined and photographed in a Nikon eclipse 80i microscope (Melville, NY), and an Olympus FV1000 confocal microscope (Tokyo, Japan), and the whole mount syringes in a Fluorescence Stereo Microscope Leica M205 FA (Wetzlar, Germany). Tracer-labeled fibers and cells in the brain, and ChAT-immunostained motor endplates in the syrinx were mapped using Neurolucida 10 (RRID:SCR_001775) in a Nikon e800 microscope equipped with a computer-controlled stage (MBF Bioscience, Williston, VT). A three-dimensional reconstruction of a syrinx displaying the localization of ChAT-labeled motor endplates was obtained by aligning contours of serial sections where the motor endplates had been marked in Neurolucida and using the solid view tool of this software. All photomicrographs were adjusted for brightness and contrast using Adobe Photoshop software and the figures were composed using Adobe Illustrator.

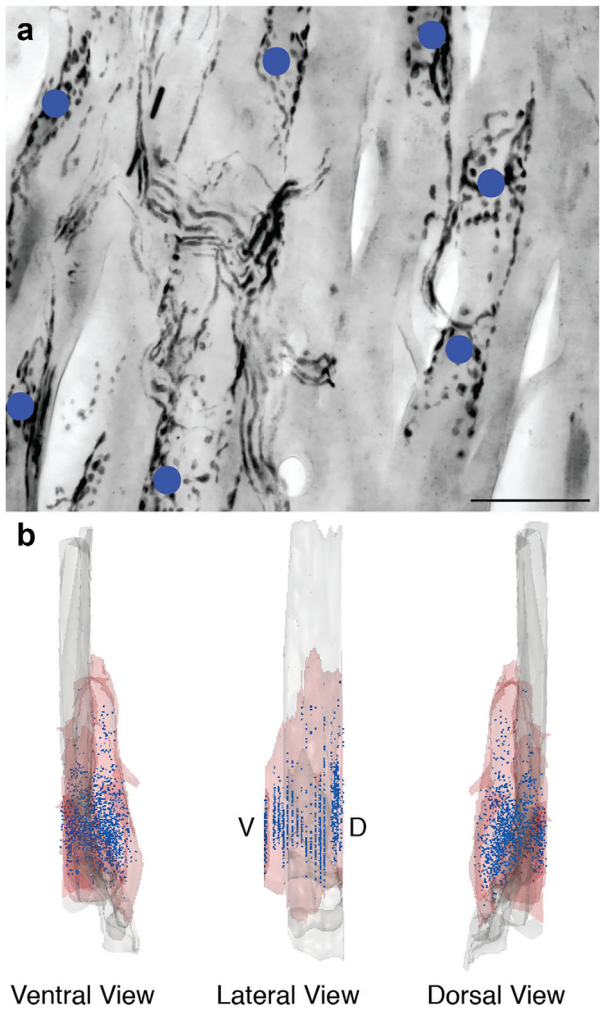

FIGURE 2 Distribution of motor endplates in the syringeal musculature. (a) Brightfield photomicrograph of a coronal section of a ChAT immunostained syrinx. Blue dots represent the markers used to reconstruct the three-dimensional distribution of motor endplates in the syringeal muscles. (b) Ventral, lateral, and dorsal view of the reconstructed syrinx. Syringeal muscles are depicted in red and the rest of the syrinx is depicted in gray. Scale bar in (a) = 50 μm

3 | RESULTS

3.1 | Immunostaining of sensory and motor fiber terminals in the syrinx

To first picture the innervation of the syrinx, we performed immunostaining against neurofilament (Figure 1c,e,f). Immunofluorescent

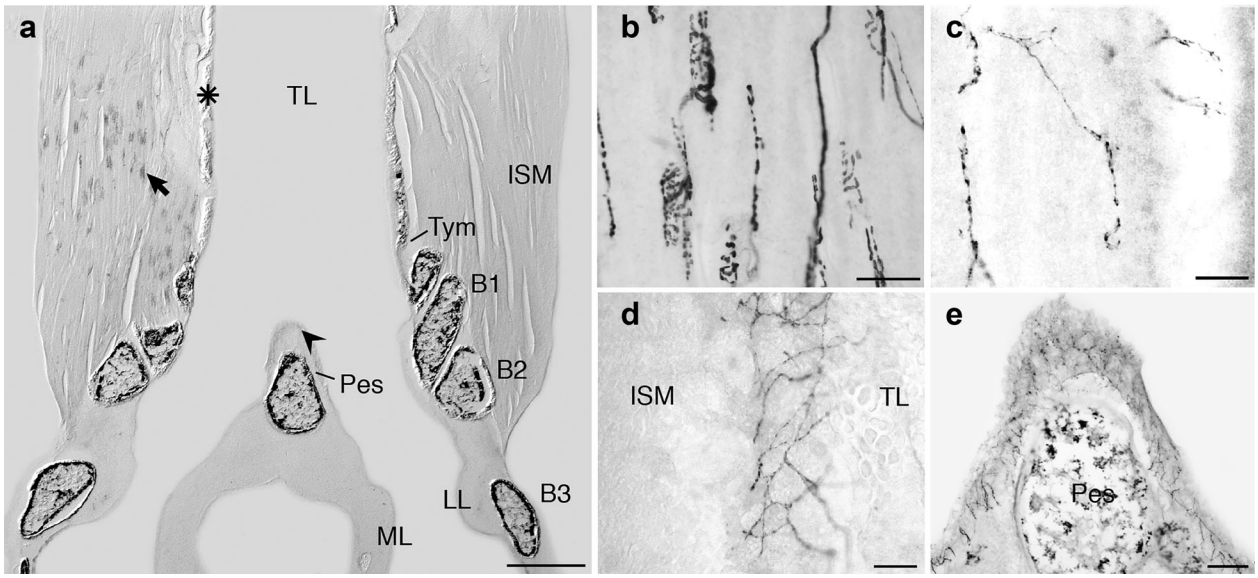

FIGURE 3 Peripheral nerve endings of syringeal receptors labeled with an in vivo injection of CTB into the tracheosyringeal nerve. (a) Low power photomicrograph of a coronal section of a syrinx immunostained against CTB. Staining of the sectioned skeletal elements is nonspecific and occurs even in the absence of primary antibody incubation. The arrow, asterisk, and arrowhead are located in the syringeal muscles, luminal wall of the trachea, and extracellular matrix-rich tissue of the pessulus, respectively, and indicate the usual location CTB labeling. (b–e) High power photomicrographs showing CTB labeling in the syringeal muscles (b and c) luminal wall of the trachea (d), and extracellular matrix-rich tissue of the pessulus (e). B1, B2, B3 = bronchial semirings 1, 2, and 3; ISM = intrinsic syringeal muscles; LL = lateral labium; ML = medial labium; Pes = pessulus; TL = tracheal lumen; Tym = tympanum. Scale bars = 500 μm in (a), 50 μm in (b), 25 μm in (c) and (d), and 100 μm in (e)

staining in whole mount cleared syringes shows that the syrinx is a highly innervated structure. The ts nerves travel rostro-caudally along both sides of the trachea, and as they reach the syrinx, they originate several branches that invade the syringeal muscles (Figure 1c,d).

Immunohistochemistry in syringeal sections shows bundles of axons branching in all the syringeal muscles (Figure 1e,f). With the exception of a few thin processes in the tracheal luminal wall, no neurofilament staining was found outside ts and the syringeal muscles.

To visualise and distinguish between the motor and sensory components of the syringeal innervation, we used immunohistochemistry and immunofluorescence against ChAT to stain motor terminals, and against substance P, calbindin, calretinin, and parvalbumin to attempt to stain the sensory endings in syringeal sections. All these antibodies produced strong staining in control brain sections (not shown, but see Logerot, Krützfeldt, Wild, & Kubke, 2011), but only ChAT and substance P antibodies produced staining in the syrinx.

Immunofluorescence and immunohistochemistry against ChAT produced staining in thick fibers that travel through the ts nerve to branch in the syringeal muscles, ending in numerous *en plaque* motor endplates (Grim, Christ, Klepáček, & Vrabcová, 1983; Ogata, 1988) (Figures 1g,h and 2a). These endings are not homogeneously distributed across the muscles, but they concentrate, especially in the ventral muscles, in a central region spanning about a third of their rostrocaudal extent, forming a band centered slightly posterior. A reconstruction obtained from serial sections of a syrinx showing the localisation of the motor endplates is depicted in Figure 2 and Supporting Information Video 1. None of the stained structures appeared as a muscle spindle, and no ChAT immunolabeling was found outside the ts nerves and the syringeal muscles.

The substance P-like immunoreactive structures in the syrinx are thin, varicose processes, that localise in the muscles, the wall of the trachea, and some of the extracellular matrix-rich membranes of the syrinx (Figure 1h–j). They do not appear to be associated with any terminal specialisation. In the muscles, these free nerve endings are less conspicuous than the motor endplates, and even though they can be found anywhere in the muscular tissue, they are most commonly located close to skeletal elements, presumably near muscle insertions, especially in the ventral half of the syrinx. Double immunofluorescence against ChAT and substance P shows that these nerve endings are not ChAT-like immunoreactive (Figure 1h). In the luminal wall of the trachea where the substance P-like immunoreactivity was most abundant, the stained fibers form a dense plexus underneath the tracheal epithelium, and extend numerous terminations to the tracheal lumen. The extracellular matrix-rich tissues in the area of the bronchi, and especially the pessulus, also contained immunoreactive free nerve endings.

3.2 | CTB tracing of peripheral and central terminals of XIIts

As another approach to visualising the peripheral terminals in the syrinx and to identify their central components, we microinjected CTB into the ts nerve. Microinjection in one ts nerve yielded unilateral CTB labeling in the ipsilateral syringeal muscles, and bilateral labeling in the

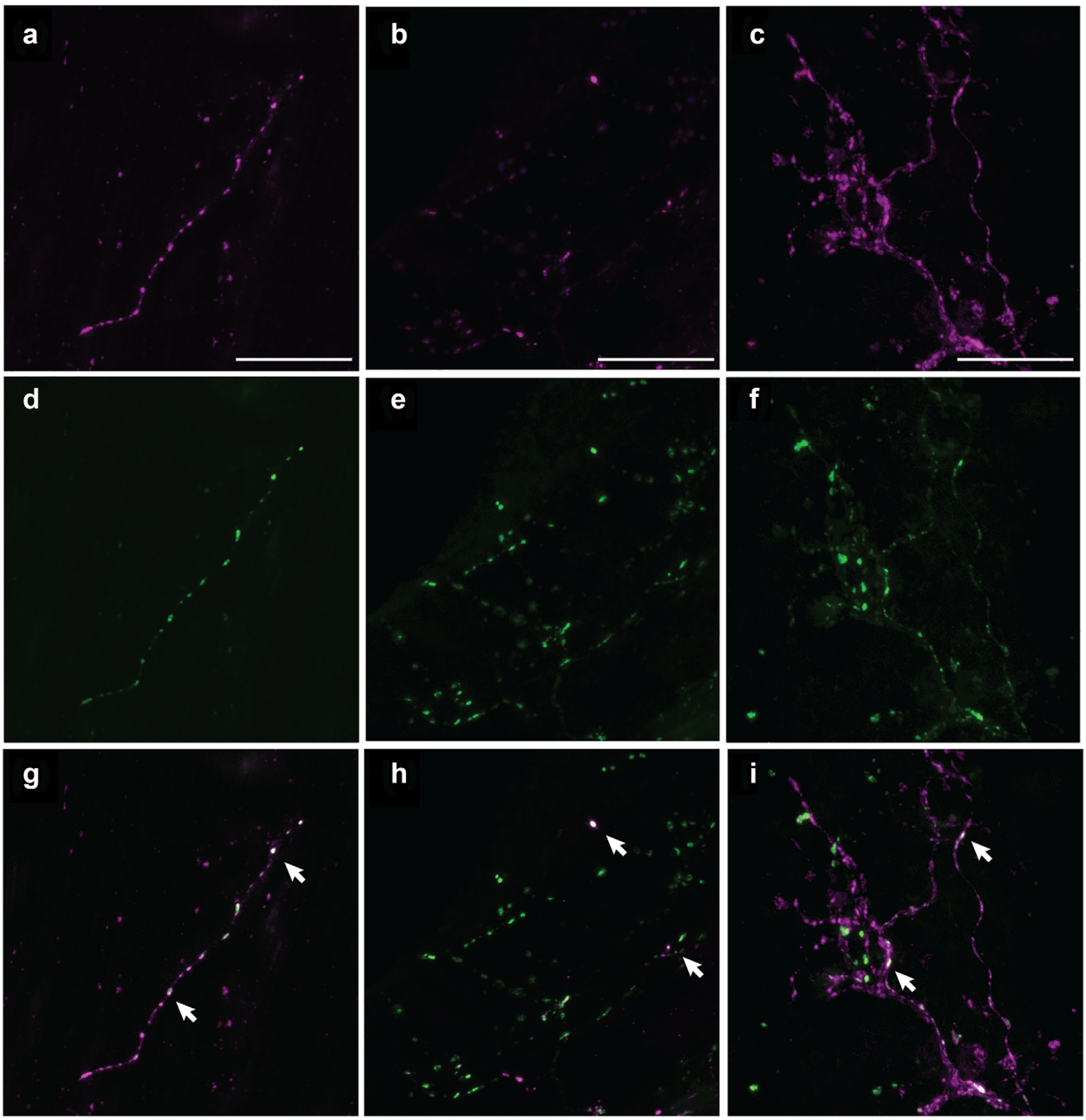

FIGURE 4 Colocalization of immunofluoresent labeling against substance P and CTB in the syrinx after a CTB injection into the tracheosyringeal nerve. High power confocal photomicrographs of coronal sections of the syrinx immunostained against CTB (pseudo-colored magenta, (a–c), substance P (green, d–f), and the merged signals (g–i); in the syringeal muscles (a, d, g), pessulus (b, e, h), and luminal wall of the trachea (c, f, i). White arrows in (g, h, i) indicate sites of colocalization of the signals. Scale bars = 25 μm

tracheal wall and syringeal cartilaginous membranes (Figure 3). CTB-labeled structures in the syrinx include motor endplate-like terminals in the tracheal and syringeal muscles (Figure 3b), identical to the ones that were previously labeled with anti-ChAT antibody, and thin and varicose processes in the muscles, luminal wall of the trachea and extracellular-matrix rich membranes (Figure 3c–e), like the structures that we previously labeled with anti-substance P antibody. Double immunofluorescence against CTB and substance P after a CTB injection in the ts nerve showed that all the thin processes labeled with CTB in the syrinx exhibited at least some substance-P-like immunoreactivity as well (Figure 4). This high degree of co-localization indicates that most, if not all, the sensory endings reaching the syrinx by the ts nerve are substance P-like immunoreactive.

The retrograde and transganglionic transport of CTB produced labeling in various parts of the brainstem, with some differences in the labeling patterns across cases. This variability is likely due to leakage of CTB from the injection site and uptake from other structures in the neck region. Nevertheless, the consistent pattern of CTB labeling of some structures allowed us to narrow down the putative central targets for sensory receptors.

Retrograde CTB labeling of cell bodies was found to a variable extent in nucleus supraspinalis and in the motor facial nuclei. In all cases

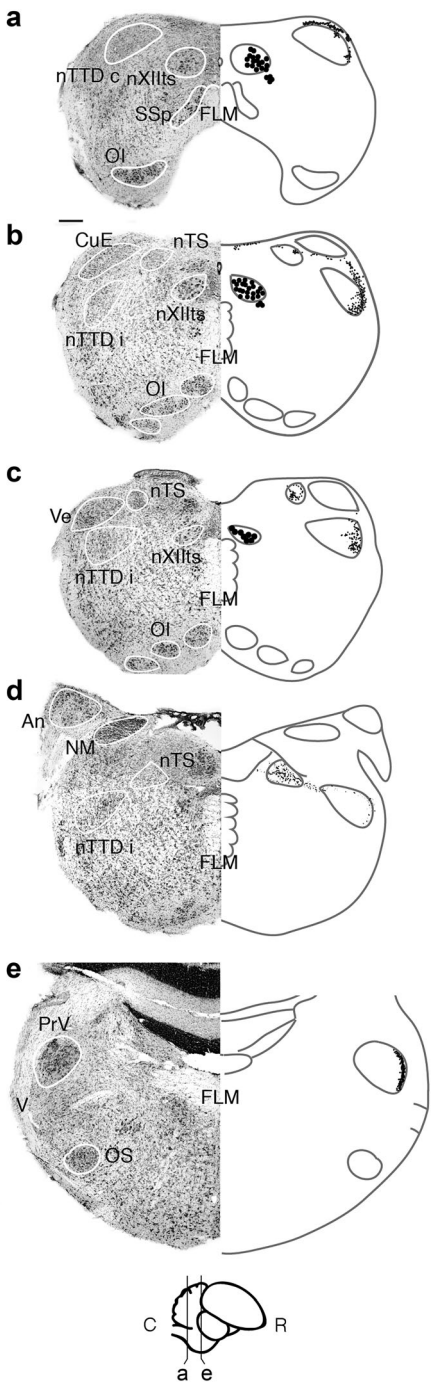

FIGURE 5 Schematic drawings of coronal sections of the brainstem, complemented with Nissl-stained material, depicting labeling in coronal sections of the brainstem after a CTB injection in the tracheosyringeal nerve. Sections separated by ~420 microns are displayed from caudal to rostral (a-e), as indicated in the inset at the bottom. Large dots represent retrogradely labeled motoneurons and small dots represent transganglionically labeled fibers and fiber endings. An = nucleus angularis; CuE = external cuneate nucleus; FLM = fasciculus longitudinalis medialis; NM = nucleus magnocellularis; nTS = nucleus of the solitary tract; nTTD c = caudal nucleus of the descending trigeminal tract; nTTD i = interpolaris nucleus of the descending trigeminal tract; nXII ts = hypoglossal tracheosyringeal motor nucleus; OI = inferior olive; OS = superior olive; PrV = principal sensory trigeminal nucleus; SSp = nucelus supraspinalis; V = trigeminal nerve root; Ve = descending vestibular nucleus. Scale bar in (a) = 200 μm (same scale in b–e)

there were labeled somata in nXIIts, as expected, and also in a smaller nucleus located just ventrolateral to nXIIts (Figures 5a–c and 6a,c).

Primary afferent terminals were transganglionically labeled in the ipsilateral sensory trigeminal nuclei (nTTD and principal nucleus [PrV]), and in the nucleus of the solitary tract (nTS). Labeling in the trigeminal complex was consistent across cases: in the nTTD, labeled terminals were located in the caudolateral part of the interpolaris subdivision (nTTDi, Faunes & Wild, 2017a), and in the principal trigeminal nucleus, it was restricted to a thin band on its lateral aspect (Figures 5 and 6), which lies just lateral to the terminal fields of the lingual branch of the hypoglossal (XII) nerve (Bottjer & Arnold, 1982; Faunes & Wild, 2017a; Wild, 1990). Labeling in the nucleus of the solitary tract was more variable. In most cases, at levels rostral to the obex, labeling could be found in different parts of the dorsoventral extent of the nucleus, in some cases bilaterally. However, at the level of the obex and just caudal and rostral to it, terminal labeling was restricted to a small dorso-lateral region ipsilateral to the injection.

Considering that most of the syringeal thin fibers labeled in the ts nerve CTB injection cases were substance P-like immunoreactive (Figure 4), it was expected that the central endings of these receptors would be immunoreactives as well. Therefore, we performed double immunofluorescence against CTB and substance P in the brainstem of these same animals (Figure 6). Both the sensory trigeminal nuclei and the nTS have substance P-like immunoreactive fiber endings. This immunoreactivity in the trigeminal sensory nuclei was coincident with, and almost restricted to, the regions of CTB labeling. In the nTS, even though there was abundant substance P-like immunoreactivity, this signal only matched consistently the location of CTB labeling in the caudolateral nTS. These results further point to the caudolateral nTTDi, lateral PrV, and caudolateral nTS as the central targets of tracheosyringeal receptors.

Having narrowed our candidate central targets, we decided to microinject CTB into the caudolateral nTTDi, lateral PrV, and caudolateral nTS, in order to find transganglionically labeled terminals in the syrinx. Three large injections that involved the caudolateral nTTDi produced labeling of thin fibers in the syrinx (Figure 7). However, in all cases, these were extremely scarce when compared to the amount of thin fiber labeling obtained with CTB injections into the ts nerve, or the amount of substance P-like immunoreactive terminals. In two of the three cases (cases 1 and 2 in Figure 7), the labeled fiber endings were seen only in the syringeal muscles, and in the third case (case 3 in Figure 7), they were also found in the tissue luminal of the pessulus. In none of the cases was found any labeling in the luminal wall of the trachea. Injections in nTS and PrV did not yield any labeling in the syrinx. However, given the scarce labeling obtained in the nTTD cases, this negative result probably should not be taken as evidence sufficient enough to refute the possibility of a projection from the syringeal receptors to these targets.

4 | DISCUSSION

In the present work, we described the motor and sensory endings in the syrinx of the zebra finch and the central terminations of the

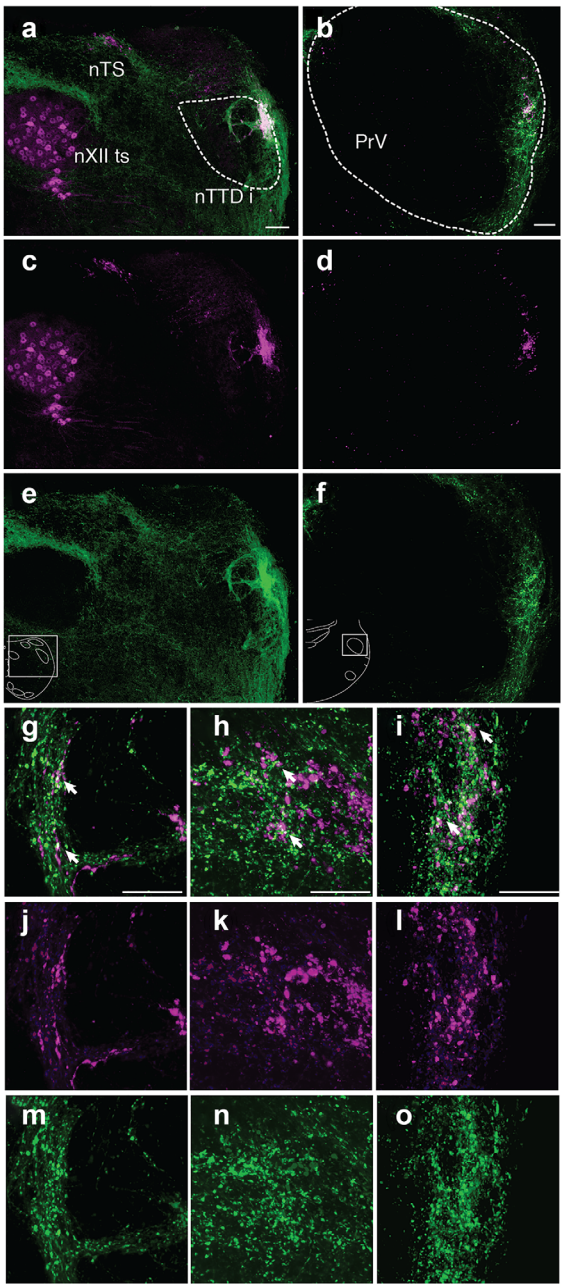

FIGURE 6 Colocalization of immunofluoresent staining against CTB and substance P in the brainstem after a CTB injection into the tracheosyringeal nerve. (a–f) Low power confocal photomicrographs of coronal sections of the brainstem immunostained against CTB (pseudo-colored magenta, c–d), substance P (green, e–f), and their merged signals (a–b), at a level just rostral to the obex (a, c, e, see inset in e), and at the level of PrV (b, d, f, see inset in f). (g–o) High power confocal photomicrographs of coronal sections of the brainstem immunostained against CTB (pseudo-colored magenta, j–l), substance P (green, m–o), and their merged signals (g–i), in the nTTD (g, j, m), nTS (h, k, n) and PrV (i, l, o). White arrows in (g, h, i) indicate sites of colocalization of the signals. nTS = nucleus of the solitary tract; nTTDi = interpolaris nucleus of the descending trigeminal tract; nXII ts = hypoglossal tracheosyringeal motor nucleus; PrV = principal sensory trigeminal nucleus. Scale bars= 100 μm in (a) (same scale in c and e); 50 μm in (b) (same scale in d and f); 25 μm in (g) (same scale in j and m), 25 μm in (h) (same scale in k and n); 25 μm in (i) (same scale in l and o)

syringeal receptors. The syringeal muscles on each side of the syrinx are innervated by the ipsilateral ts nerve. The ts nerves branch as they reach the intrinsic syringeal muscles, which contain numerous, thick, ChAT-like immunoreactive axons, and *en plaque* endplates. The localisation of these endplates is for the most part restricted to a zone that spans about a third of the length of the muscles in the rostro-caudal axis. In the syringeal muscles, we also found thin, varicose, substance P-like immunoreactive free nerve endings. Similar sensory endings were found in the tracheal luminal wall and in the internal extracellular matrix-rich tissues, especially luminal to the pessulus. Transganglionic transport of CTB showed that these receptors target a caudolateral region of the nTTDi, a caudolateral region of the nTS and a lateral band in the hypoglossal-recipient subdivision of PrV.

4.1 | Comparison to previous findings: technical considerations

The location of syringeal motoneurons in the caudal part of the hypoglossal nucleus has been known since the ts nerve lesion experiments performed by Nottebohm et al. (1976) in the canary. In all of our tracing experiments, we obtained strong somata labeling in this nucleus, but in most of them we also obtained variable labeling in other motor nuclei, particularly in the small nucleus located ventrolateral to XIIts. Both nXIIts and the group of cells ventrolateral to nXIIts were also labeled by Bottjer and Arnold (1982) in the zebra finch and by Wild (1981) in the cockatoo by applying HRP crystals to the severed ts nerve near its separation from the lingual hypoglossal branch. However, only XIIts motoneurons were labeled when wheat germ agglutinin was injected into the ventral syringeal muscles (Bottjer & Arnold, 1982; Wild, 1981), supporting the idea that the ventrolateral nucleus projects to extrinsic tracheosyringeal muscles (Wild, 1981). Cells in a similar ventrolateral position have been traced in the fowl from injections into the ypsilotrachealis or cleidotrachealis muscle (Youngren & Philips, 1983), a muscle that originates on the clavicle, inserts into the upper trachea (George & Berger, 1966), and is active during phonation (Youngren, Peek, & Phillips, 1974). In passerines, this muscle also inserts in the rostral trachea, far from the syrinx (Shufeldt, 1890 in the raven; personal observations in the zebra finch), but a role in vocalization seems unlikely because, unlike XIIts motoneurons, the motoneurons ventrolateral to XIIts that probably innervate this muscle do not receive a descending projection from the telencephalic song control system (Wild, 1993).

HRP application to the ts nerve (Bottjer & Arnold, 1982) showed that the cell bodies of ts afferents lie in the jugular vagal ganglion, as are the cell bodies of the mechanoreceptors in the tongue (Wild, 1990). However, in Bottjer and Arnold's experiments, HRP failed to transport trans-ganglionically and therefore the specific central targets of the tracheosyringeal receptors could not be identified. Only by making injections into the main trunk of the hypoglossal nerve, central to its separation into lingual and tracheosyringeal branches, were they able to obtain transganglionic transport and chart the hypoglossal terminal fields in the brainstem, presumably including both lingual and tracheosyringeal afferents. In the present work, the use of CTB as a more

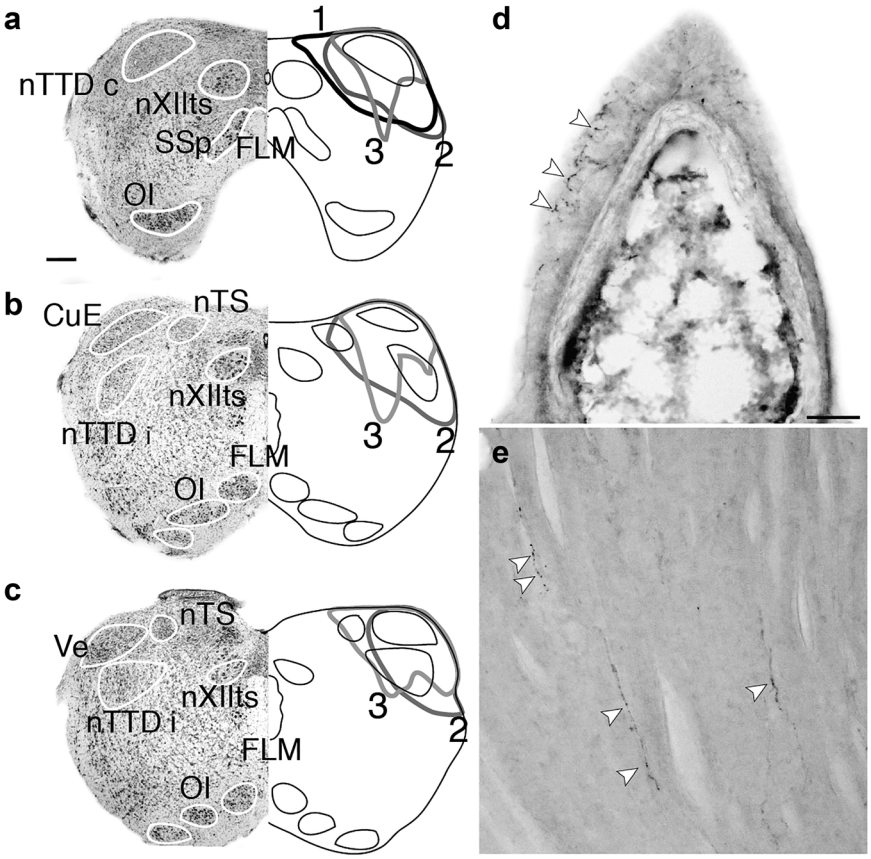

FIGURE 7 CTB injections in the nTTD produce labeling of sensory endings in the syrinx. (a–c) Schematic drawings of coronal sections of the brainstem, complemented with Nissl-stained material, depicting CTB injection sites in three different cases. (d, e) Photomicrographs of coronal sections of the syrinx showing CTB labeled fibers in the tissue luminal to the pessulus after injection N° 3 (d) and in the syringeal muscles after injection N° 2 (e). Abbreviations as in Figure 5. Scale bar in (a) = 200 μm (same scale in b and c), scale bar in (d) = 50 μm (same scale in e)

sensitive transganglionic tracer allowed us to distinguish the specific tracheosyringeal terminal fields. However, CTB is easily taken up by tissue near the injection site and can therefore produce nonspecific labeling. Nevertheless, the consistent labeling of the lateral nTTD, nTS, and PrV across cases and their coincident immunolabeling with a substance P antibody allows us to identify these three structures as the most probable central targets of tracheosyringeal receptors. Transganglionic transport of CTB from the brainstem to the syrinx was attempted as another approach to overcome the problem of tracer leakage from peripheral nerve injections. However, tracer transport in this direction proved to be much reduced, as evidenced by the small amount of labeling obtained in the syrinx in the cases where there was any, compared to the robust labeling obtained from ts nerve injections. Nevertheless, the approach using central injections allowed us to confirm unequivocally the projection from the syrinx to the lateral nTTD. We do not consider the absence of syringeal labeling following nTS and PrV injections as sufficient evidence to rule out possible projections to these targets.

The central projections of the tracheosyringeal receptors described here represent a small portion of the previously described hypoglossal terminal fields, most of which derive from lingual mechanoreceptors, and include a continuous rostro-caudal column spanning the brainstem from the medial cervical dorsal column to the lateral half of PrV (Bottjer & Arnold, 1982; Faunes & Wild, 2017a; Wild, 1990). A hypoglossal projection to the lateral region of the nTS has also been described for the lingual nerve by Wild (1990), but not by Bottjer & Arnold (1982). In pigeons and songbirds, the lateral parasolitary nucleus of nTS (lPs) has also been shown to receive pulmonary afferents (Katz & Karten, 1983; Wild, 2004).

4.2 | Motor innervation of the syringeal muscles

It has been shown that in avian muscles, fast twitching fibers differ from slow tonic fibers in that the former are innervated by a single motoneuron that contacts them at a single motor endplate with an *en plaque* morphology, while the latter receive numerous *en grappe* endings that originate from many motoneurons (George & Berger, 1966). We visualised the motor endplates in the syringeal muscles by ChAT immunolabeling and CTB tracing. In coronal sections of the syrinx, these endplates looked like *en plaque* endplates previously described by Chinoy and George (1965) and Grim et al. (1983), which is consistent with the extremely fast contraction rates exhibited by the syringeal muscles (Elemans, Mead, Rome, & Goller, 2008). In dissociated fibers from zebra finch intrinsic syringeal muscles, Bleisch, Scharff, and

Nottebohm (1989) visualised the location of motor endplates using alpha bungarotoxin conjugated to fluorescein isothiocyanate, and found that most of the fibers exhibited a single motor endplate, but all muscles had a certain number of multiply innervated fibers. Therefore, it is possible that the zebra finch syrinx has a small proportion of *en grappe* endplates, which we could not identify in our material because of the steric constrains associated with sectioned tissue. Nevertheless, our description of the overall restricted rostrocaudal distribution of motor endplates, forming a single band in most anteroposterior levels—and likely spanning the whole length of the muscle (see Donovan et al., 2012)—is consistent with a high proportion of focally innervated fibers. In turn, these findings, together with recent descriptions of zebra finch syringeal muscle morphology (Düring et al., 2013), could be useful in future research on the biomechanics of sound production and motor control in this system (Elemans et al., 2015).

In the present work and in agreement with Bleisch et al. (1989) and Wild and Suthers (unpublished observations in various songbird species), we did not find any evidence of muscle spindles in any of the syringeal muscles. Furthermore, Duc, Barakat-Walter, and Droz (1993) found calbindin immunopositive axons innervating spindles in chicken hindlimb muscles, whereas in the syringeal muscles, we did not find any calbindin immunoreactivity.

4.3 | Sensory innervation of the syrinx

The absence of spindles in the syringeal muscles raises the question as to what modalities are involved in syringeal sensory feedback. Our finding of substance P-like immunoreactivity in sensory endings in the syrinx is consistent with the substance-P like immunoreactivity previously reported for the jugular ganglion in pigeons (Katz & Karten, 1980). Thin, varicose, substance P-like immunoreactive nerve endings like the ones we found in the syringeal muscles have previously been seen in chicken hindlimb muscles and skin (Duc et al., 1993). However, their sensory modality is presently unknown. These muscular sensory endings, along with the endings in the tissue luminal to the pessulus, were shown to belong to nTTDi projecting receptors. Furthermore, their location near muscle insertions and flexible tissue is suggestive of a mechanosensory function. The skeletal muscles of mammals also have free nerve endings originating from thin afferent fibers, which can respond to muscle contraction and stretch, as well as to thermal and chemical stimuli (Cleland, Hayward, & Rymer, 1990; Kniffki, Mense, & Schmidt, 1978; Kumazawa & Mizumura, 1977; Stacey, 1969). Future studies examining the expression of ion channels (e.g., piezo proteins, Coste et al., 2010) and the neurophysiology of these receptors will be needed to solve this question.

The sensory endings in the luminal tracheal wall were not transganglionically labeled by any of our brainstem injections, which we consider to be due to inefficient tracer transport. In the tracheal wall of mammals, there is a substance P immunopositive nervous plexus originating from jugular ganglion neurons similar to the ones we describe here (Mazzone & Undem, 2016). These jugular neurons project to the paratrigeminal nucleus and to the nucleus of the solitary tract (McGovern et al., 2015). Like the mammalian trachea and broncho-pulmonary system in general, the avian trachea and air sacs also receive an innervation via the nodose ganglion (Bower, Parker, & Molony, 1978; Kubke, Ross, & Wild, 2004).

4.4 | Syringeal feedback to the song system?

As in human speech, the role of auditory feedback in bird singing has received far more attention than the role of somatosensory or proprioceptive feedback (Konishi, 2004; Suthers, Goller, & Wild, 2002). However, while it is clear that the mammalian vocal organ is highly innervated with different kinds of mechanoreceptors that play a role in human speech (reviewed in Jürgens, 2002), evidence for a syringeal somatosensory feedback to the song system has remained more elusive. Bottjer & Arnold (1984) tested the effects of syringeal deafferentation on adult song production and reported that this procedure had almost no influence on singing. However, the time range evaluated in this study was shorter than the time deafening takes to produce an effect on adult song (Nordeen & Nordeen, 1992). Furthermore, the role of syringeal somatosensory feedback in song learning has not yet been evaluated and, like auditory feedback, its contribution to this process might be more evident than to adult song maintenance. In point of fact, Bottjer and To (2012) showed singing-induced Fos expression in part of the hypoglossal recipient trigeminal complex of juvenile zebra finches, and found that vagal and hypoglossal denervation impairs juvenile singing to varying degrees. Furthermore, vagal feedback from other parts of the respiratory system has been shown to be important in the motor control of singing in adult birds (Méndez, Dall'asén, & Goller, 2010).

In our current understanding of the song system, bottom-up connections originating from the respiratory and vocal centres in the brainstem appear to play a major role in the operation of the circuit (Alonso, Trevisan, Amador, Goller, & Mindlin, 2015; Ashmore, Renk, & Schmidt, 2008; Schmidt & Wild, 2014). The present description of the central projections of the syringeal receptors constitutes a step in elucidating the possible connections between syringeal sensory feedback and the song system. Vocalisation and respiration are highly integrated functions in songbirds (Hartley, 1990), and therefore it is likely that the projection from the syrinx to the nTS serves a function in both processes. Furthermore, the projection to nTTDi could reach the song system via nucleus uvaeformis (Uva) of the dorsal thalamus (Faunes & Wild, 2017b), which mediates the projections from respiratory and vocal centres to the forebrain nuclei of the song system (Ashmore et al., 2008; Wild, 1994).

ACKNOWLEDGMENTS

The confocal imaging for this work was performed at the Biomedical Imaging Research Unit of the Faculty of Medical and Health Sciences of the University of Auckland. We thank Rashi C. Karunasinghe and Pablo Henny for their kind help in some steps of this work.

CONFLICT OF INTEREST STATEMENT

The authors declare that there is no actual or potential conflict of interest in relation to this article.

ROLE OF AUTHORS

All authors had full access to all the data in the study and take responsibility for the integrity of the data and the accuracy of the data analysis. Study concept and design: MF, JMW. Acquisition of data: MF, JFB, JMW. Analysis and interpretation of data: MF, JFB, JMW. Drafting of the manuscript: MF. Critical revision of the manuscript for important intellectual content: JFB, JMW. Obtained funding: JMW. Study supervision: JMW.

REFERENCES

Alonso, R. G., Trevisan, M. A., Amador, A., Goller, F., & Mindlin, G. B. (2015). A circular model for song motor control in Serinus canaria. *Frontiers in Computational Neuroscience*, *9*, 41. doi:10.3389/fncom.2015.00041

Ames, P. L. (1971). *The morphology of the syrinx in passerine birds* (Vol. 37). Peabody Museum of Natural History, Yale University, CT.

Ashmore, R. C., Renk, J. A., & Schmidt, M. F. (2008). Bottom-up activation of the vocal motor forebrain by the respiratory brainstem. *Journal of Neuroscience*, *28*(10), 2613–2623. doi:10.1523/JNEUROSCI.4547-07.2008

Bleisch, W., Scharff, C., & Nottebohm, F. (1989). Neural cell adhesion molecule (N-CAM) is elevated in adult avian slow muscle fibers with multiple terminals. *Proceedings of the National Academy of Sciences of the United States of America*, *86*(16), 6403–6407.

Botelho, J. F., Smith-Paredes, D., Soto-Acuña, S., Núñez-León, D., Palma, V., & Vargas, A. O. (2017). Greater growth of proximal metatarsals in bird embryos and the evolution of hallux position in the grasping foot. *Journal of Experimental Zoology Part B: Molecular and Developmental Evolution*, *328*(1–2), 106–118. doi:10.1002/jez.b.22697

Bottjer, S. W., & Arnold, A. P. (1982). Afferent neurons in the hypoglossal nerve of the zebra finch (Poephila guttata): Localization with horseradish peroxidase. *Journal of Comparative Neurology*, *210*(2), 190–197. doi:10.1002/cne.902100209

Bottjer, S. W., & Arnold, A. P. (1984). The role of feedback from the vocal organ. I. Maintenance of stereotypical vocalizations by adult zebra finches. *Journal of Neuroscience*, *4*(9), 2387–2396.

Bottjer, S. W., & To, M. (2012). Afferents from vocal motor and respiratory effectors are recruited during vocal production in juvenile songbirds. *Journal of Neuroscience*, *32*(32), 10895–10906. doi:10.1523/JNEUROSCI.0990-12.2012

Bower, A. J., Parker, S., & Molony, V. (1978). An autoradiographic study of the afferent innervation of the trachea, syrinx and extrapulmonary primary bronchus of Gallus gallus domesticus. *Journal of Anatomy*, *126*(Pt 1), 169–180.

Braun, K. (1990). Calcium-binding proteins in avian and mammalian central nervous system: Localization, development and possible functions. *Progress in Histochemistry and Cytochemistry*, *21*(1), III–V, 1–62. doi:10.1016/S0079-6336(11)80044-6

Celio, M. R., Baier, W., Schärer, L., De Viragh, P. A., & Gerday, C. H. (1988). Monoclonal antibodies directed against the calcium binding protein parvalbumin. *Cell Calcium*, *9*(2), 81–86. doi:10.1016/0143-4160(88)90027-9

Chinoy, N. J., & George, J. C. (1965). Cholinesterases in the pectoral muscle of some vertebrates. *The Journal of physiology*, *177*(3), 346.

Cleland, C. L., Hayward, L., & Rymer, W. Z. (1990). Neural mechanisms underlying the clasp-knife reflex in the cat. II. Stretch-sensitive muscular-free nerve endings. *Journal of Neurophysiology*, *64*(4), 1319–1330.

Coste, B., Mathur, J., Schmidt, M., Earley, T. J., Ranade, S., Petrus, M. J., … Patapoutian, A. (2010). Piezo1 and Piezo2 are essential components of distinct mechanically activated cation channels. *Science*, *330*(6000), 55–60. doi:10.1126/science.1193270

Donovan, E. R., Keeney, B. K., Kung, E., Makan, S., Wild, J. M., & Altshuler, D. L. (2012). Muscle activation patterns and motor anatomy of Anna's hummingbirds Calypte anna and zebra finches Taeniopygia guttata. *Physiological and Biochemical Zoology*, *86*(1), 27–46.

Doupe, A. J., & Kuhl, P. K. (1999). Birdsong and human speech: Common themes and mechanisms. *Annual Review of Neuroscience*, *22*(1), 567–631. doi:10.1146/annurev.neuro.22.1.567

Duc, C., Barakat-Walter, I., & Droz, B. (1993). Calbindin D-28k-and substance P-immunoreactive primary sensory neurons: Peripheral projections in chick hindlimbs. *Journal of Comparative Neurology*, *334*(1), 151–158. doi:10.1002/cne.903340112

Düring, D. N., Ziegler, A., Thompson, C. K., Ziegler, A., Faber, C., Müller, J., … Elemans, C. P. (2013). The songbird syrinx morphome: A three-dimensional, high-resolution, interactive morphological map of the zebra finch vocal organ. *BMC Biology*, *11*(1), 1. doi:10.1186/1741-7007-11-1

Elemans, C. P. (2014). The singer and the song: The neuromechanics of avian sound production. *Current Opinion in Neurobiology*, *28*, 172–178. doi:10.1016/j.conb.2014.07.022

Elemans, C. P., Mead, A. F., Rome, L. C., & Goller, F. (2008). Superfast vocal muscles control song production in songbirds. *PLoS One*, *3*(7), e2581. doi:10.1371/journal.pone.0002581

Elemans, C. P. H., Rasmussen, J. H., Herbst, C. T., Düring, D. N., Zollinger, S. A., Brumm, H., … Sober, S. J. (2015). Universal mechanisms of sound production and control in birds and mammals. *Nature Communications*, *6*, 8978. doi:10.1038/ncomms9978

Faunes, M., & Wild, J. M. (2017a). The sensory trigeminal complex and the organisation of its primary afferents in the zebra finch (*Taeniopygia guttata*). *J Comp Neurol*. doi:10.1002/cne.24249

Faunes, M., & Wild, J. M. (2017b). The ascending projections of the nuclei of the descending trigeminal tract (nTTD) in the zebra finch (*Taenopygia guttata*). *J Comp Neurol*. doi:10.1002/cne.24247

Fee, M. S., Shraiman, B., Pesaran, B., & Mitra, P. P. (1998). The role of nonlinear dynamics of the syrinx in the vocalizations of a songbird. *Nature*, *395*(6697), 67–71. doi:10.1038/25725

George, J. C., & Berger, A. J. (1966). *Avian myology*. New York, NY: Academic Press.

Goller, F., & Cooper, B. G. (2004). Peripheral motor dynamics of song production in the zebra finch. *Annals of the New York Academy of Sciences*, *1016*(1), 130–152. doi:10.1196/annals.1298.009

Goller, F., & Larsen, O. N. (1997). A new mechanism of sound generation in songbirds. *Proceedings of the National Academy of Sciences of the United States of America*, *94*(26), 14787–14791.

Goller, F., & Suthers, R. A. (1996). Role of syringeal muscles in controlling the phonology of bird song. *Journal of Neurophysiology*, *76*(1), 287–300.

Grant, B. R., & Grant, P. R. (2010). Songs of Darwin's finches diverge when a new species enters the community. *Proceedings of the National Academy of Sciences of the United States of America*, *107*(47), 20156–20163. doi:10.1073/pnas.1015115107

Grim, M., Christ, B., Klepáček, I., & Vrabcová, M. (1983). A comparison of motor end-plate distribution and the morphology of some wing muscles of the chick and quail. *The Histochemical Journal*, *15*(4), 289–291. doi:10.1007/BF01002950

Hartley, R. S. (1990). Expiratory muscle activity during song production in the canary. *Respiration physiology*, *81*(2), 177–187. doi:10.1016/0034-5687(90)90044-Y

Hirokawa, N., Glicksman, M. A., & Willard, M. B. (1984). Organization of mammalian neurofilament polypeptides within the neuronal cytoskeleton. *The Journal of Cell Biology*, *98*(4), 1523–1536.

Hokfelt, T., Kellerth, J. O., Nilsson, G., & Pernow, B. (1975). Substance P: Localization in the central nervous system and in some primary sensory neurons. *Science*, *190*(4217), 889–890. doi:10.1126/science.242075

Houser, C. R., Crawford, G. D., Barber, R. P., Salvaterra, P. M., & Vaughn, J. E. (1983). Organization and morphological characteristics of cholinergic neurons: An immunocytochemical study with a monoclonal antibody to choline acetyltransferase. *Brain Research*, *266*(1), 97–119. doi:10.1016/0006-8993(83)91312-4

Jürgens, U. (2002). Neural pathways underlying vocal control. *Neuroscience & Biobehavioral Reviews*, *26*(2), 235–258. doi:10.1016/S0149-7634(01)00068-9

Katz, D. M., & Karten, H. J. (1980). Substance P in the vagal sensory ganglia: Localization in cell bodies and pericellular arborizations. *Journal of Comparative Neurology*, *193*(2), 549–564. doi:10.1002/cne.901930216

Katz, D. M., & Karten, H. J. (1983). Visceral representation within the nucleus of the tractus solitarius in the pigeon, Columba livia. *Journal of Comparative Neurology*, *218*(1), 42–73. doi:10.1002/cne.902180104

King, A. (1989). Functional anatomy of the syrinx. In A. King & J. Mclelland (Eds.), *Form and function in birds* (Vol. *4*, pp. 105–192). London, England: Academic Press.

Kniffki, K. D., Mense, S., & Schmidt, R. F. (1978). Responses of group IV afferent units from skeletal muscle to stretch, contraction and chemical stimulation. *Experimental Brain Research*, *31*(4), 511–522. doi:10.1007/BF00239809

Konishi, M. (2004). The role of auditory feedback in birdsong. *Annals of the New York Academy of Sciences*, *1016*(1), 463–475. doi:10.1196/annals.1298.010

Kubke, M. F., Ross, J. M., & Wild, J. M. (2004). Vagal innervation of the air sacs in a songbird, Taenopygia guttata. *Journal of Anatomy*, *204*(4), 283–292. doi:10.1111/j.0021-8782.2004.00286.x

Kumazawa, T., & Mizumura, K. (1977). Thin-fibre receptors responding to mechanical, chemical, and thermal stimulation in the skeletal muscle of the dog. *The Journal of Physiology*, *273*(1), 179–194.

Lee, V. M. Y., Carden, M. J., Schlaepfer, W. W., & Trojanowski, J. Q. (1987). Monoclonal antibodies distinguish several differentially phosphorylated states of the two largest rat neurofilament subunits (NF-H and NF-M) and demonstrate their existence in the normal nervous system of adult rats. *Journal of Neuroscience*, *7*(11), 3474–3488.

Logerot, P., Krützfeldt, N. O., Wild, J. M., & Kubke, M. F. (2011). Subdivisions of the auditory midbrain (n. mesencephalicus lateralis, pars dorsalis) in zebra finches using calcium-binding protein immunocytochemistry. *PLoS One*, *6*(6), e20686. doi:10.1371/journal.pone.0020686

Marler, P. (1970). A comparative approach to vocal learning: Song development in white-crowned sparrows. *Journal of Comparative and Physiological Psychology*, *71*(2p2), 1. doi:10.1037/h0029144

Marler, P. (2004). *Science and birdsong: The good old days. In Nature's music: The science of birdsong* (pp. 1–38). Marler P. and Slabbekoorn H. S. (Eds.), Dordrecht, The Netherlands: Elsevier.

Mazzone, S. B., & Undem, B. J. (2016). Vagal afferent innervation of the airways in health and disease. *Physiological Reviews*, *96*(3), 975–1024. doi:10.1152/physrev.00039.2015

McGovern, A. E., Driessen, A. K., Simmons, D. G., Powell, J., Davis-Poynter, N., Farrell, M. J., & Mazzone, S. B. (2015). Distinct brainstem and forebrain circuits receiving tracheal sensory neuron inputs revealed using a novel conditional anterograde transsynaptic viral tracing system. *Journal of Neuroscience*, *35*(18), 7041–7055. doi:10.1523/JNEUROSCI.5128-14.2015

Méndez, J. M., Dall'asén, A. G., & Goller, F. (2010). Disrupting vagal feedback affects birdsong motor control. *Journal of Experimental Biology*, *213*(24), 4193–4204. doi:10.1242/jeb.045369

Nordeen, K. W., & Nordeen, E. J. (1992). Auditory feedback is necessary for the maintenance of stereotyped song in adult zebra finches. *Behavioral and Neural Biology*, *57*(1), 58–66. doi:10.1016/0163-1047(92)90757-U

Nottebohm, F., Stokes, T. M., & Leonard, C. M. (1976). Central control of song in the canary, Serinus canarius. *Journal of Comparative Neurology*, *165*(4), 457–486. doi:10.1002/cne.901650405

Ogata, T. (1988). Structure of motor endplates in the different fiber types of vertebrate skeletal muscles. *Archives of Histology and Cytology*, *51*(5), 385–424. doi:10.1679/aohc.51.385

Prum, R. O. (1992). *Syringeal morphology, phylogeny, and evolution of the neotropical manakins (Aves: Pipridae). American Museum Novitates*, *3043*, 1–65.

Riede, T., & Goller, F. (2010). Functional morphology of the sound-generating labia in the syrinx of two songbird species. *Journal of Anatomy*, *216*(1), 23–36. doi:10.1111/j.1469-7580.2009.01161.x

Schmidt, M. F., & Wild, J. M. (2014). The respiratory-vocal system of songbirds: Anatomy, physiology, and neural control. *Progress in Brain Research*, *212*, 297. doi:10.1016/B978-0-444-63488-7.00015-X

Shufeldt, R. W. (1890). *The myology of the raven (Corvus corax sinuatus.): A guide to the study of the muscular system in birds*. London and New York: Macmillan and Company.

Stacey, M. J. (1969). Free nerve endings in skeletal muscle of the cat. *Journal of Anatomy*, *105*(Pt 2), 231.

Stensrud, M. J., Chaudhry, F. A., Leergaard, T. B., Bjaalie, J. G., & Gundersen, V. (2013). Vesicular glutamate transporter-3 in the rodent brain: Vesicular colocalization with vesicular γ-aminobutyric acid transporter. *Journal of Comparative Neurology*, *521*(13), 3042–3056. doi:10.1002/cne.23331

Suthers, R. A., Goller, F., & Wild, J. M. (2002). Somatosensory feedback modulates the respiratory motor program of crystallized birdsong. *Proceedings of the National Academy of Sciences of the United States of America*, *99*(8), 5680–5685. doi:10.1073/pnas.042103199

Suthers, R. A., & Zollinger, S. A. (2004). Producing song: The vocal apparatus. *Annals of the New York Academy of Sciences*, *1016*(1), 109–129. doi:10.1196/annals.1298.041

Tomer, R., Ye, L., Hsueh, B., & Deisseroth, K. (2014). Advanced CLARITY for rapid and high-resolution imaging of intact tissues. *Nature Protocols*, *9*(7), 1682–1697. doi:10.1038/nprot.2014.123

Wild, J. M. (1981). Identification and localization of the motor nuclei and sensory projections of the glossopharyngeal, vagus, and hypoglossal nerves of the cockatoo (Cacatua roseicapilla), Cacatuidae. *Journal of Comparative Neurology*, *203*(3), 351–377. doi:10.1002/cne.902030304

Wild, J. M. (1990). Peripheral and central terminations of hypoglossal afferents innervating lingual tactile mechanoreceptor complexes in Fringillidae. *Journal of Comparative Neurology*, *298*(2), 157–171. doi:10.1002/cne.902980203

Wild, J. M. (1993). Descending projections of the songbird nucleus robustus archistriatalis. *Journal of Comparative Neurology*, *338*(2), 225–241. doi:10.1002/cne.903380207

Wild, J. M. (1994). Visual and somatosensory inputs to the avian song system via nucleus uvaeformis (Uva) and a comparison with the

projections of a similar thalamic nucleus in a nonsongbird, *columbia livia*. *Journal of Comparative Neurology*, *349*(4), 512–535. doi:10.1002/cne.903490403

Wild, J. M. (2004). Functional neuroanatomy of the sensorimotor control of singing. *Annals of the New York Academy of Sciences*, *1016*(1), 438–462. doi:10.1196/annals.1298.016

Wild, J. M. (2008). Birdsong: Anatomical foundations and central mechanisms of sensorimotor integration. In H. P. Zeigler & P. Marler (Eds.), *Neuroscience of birdsong* (pp. 136–152). UK: Cambridge University Press.

Yan, Y., Jensen, K., & Brown, A. (2007). The polypeptide composition of moving and stationary neurofilaments in cultured sympathetic neurons. *Cell Motility and the Cytoskeleton*, *64*(4), 299. doi:10.1002/cm.20184

Youngren, O. M., Peek, F. W., & Phillips, R. E. (1974). Repetitive vocalizations evoked by local electrical stimulation of avian brains. III. Evoked activity in the tracheal muscles of the chicken (Gallus gallus). *Brain, Behavior and Evolution*, *9*(6), 393–421.

Youngren, O. M., & Philips, R. E. (1983). Location and distribution of tracheosyringeal motorneuron somata in the fowl. *Journal of Comparative Neurology*, *213*(1), 86–93. doi:10.1002/cne.902130108

Zimmermann, L., & Schwaller, B. (2002). Monoclonal antibodies recognizing epitopes of calretinins: Dependence on Ca2+-binding status and differences in antigen accessibilityin colon cancer cells. *Cell Calcium*, *31*(1), 13–25. doi:10.1054/ceca.2001.0255

SUPPORTING INFORMATION

Additional Supporting Information may be found online in the supporting information tab for this article.

Video 1. Rotation of a Neurolucida three-dimensional reconstruction of half a syrinx. Syringeal cartilagues are displayed in gray and syringeal intrinsic muscles are displayed in red. Blue dots indicate the location of ChAT-like immunopositive motor end plates. Green arrow points rostrally, blue arrow points dorsally, and red arrow points medially.

How to cite this article: Faunes M, Botelho JF, Wild JM. Innervation of the syrinx of the zebra finch (*Taeniopygia guttata*). *J Comp Neurol*. 2017;00:000–000. https://doi.org/10.1002/cne.24236